

NJC

Accepted Manuscript



This is an *Accepted Manuscript*, which has been through the Royal Society of Chemistry peer review process and has been accepted for publication.

Accepted Manuscripts are published online shortly after acceptance, before technical editing, formatting and proof reading. Using this free service, authors can make their results available to the community, in citable form, before we publish the edited article. We will replace this *Accepted Manuscript* with the edited and formatted *Advance Article* as soon as it is available.

You can find more information about *Accepted Manuscripts* in the [Information for Authors](#).

Please note that technical editing may introduce minor changes to the text and/or graphics, which may alter content. The journal's standard [Terms & Conditions](#) and the [Ethical guidelines](#) still apply. In no event shall the Royal Society of Chemistry be held responsible for any errors or omissions in this *Accepted Manuscript* or any consequences arising from the use of any information it contains.

ARTICLE

Hydrothermal Synthesis of BaZrO₃ Fine Particles Controlled in Size and Shape and Fluorescence Behavior by Europium Doping

Cite this: DOI: 10.1039/x0xx00000x

Received 00th January 2012,
Accepted 00th January 2012

DOI: 10.1039/x0xx00000x

www.rsc.org/

Kiyoshi Kanie,* Yuki Seino, Masaki Matsubara, Masafumi Nakaya, and Atsushi Muramatsu

Monodispersed barium zirconate (BaZrO₃) fine particles with high crystallinity have been synthesized by hydrothermal reactions using barium hydroxide and a Zr-triethanolamine complex. The particle shape was controlled by change of initial Ba²⁺ and Zr⁴⁺ concentrations, and sphere-, rhombic dodecahedral-, and flower-shaped BaZrO₃ fine particles were obtained. On the other hand, the particle mean size of the BaZrO₃ microspheres was precisely controlled by the addition of NaOH into the precursor solutions. By Eu-doping, the present BaZrO₃ synthesis was also applied to investigate the effect of size and shape on the fluorescence properties as a phosphor. The asymmetric ratio of the photoluminescence intensity of the resulting Eu-doped BaZrO₃ powders suggested the particles obtained by the present method had a basically single crystalline structure.

1. Introduction

Barium zirconate (BaZrO₃) has unique material features such as high melting point,¹⁾ small thermal expansion coefficient,¹⁾ wide band gap,²⁾ and high dielectric permittivity.^{3,4)} BaZrO₃ is widely used as a key material for industrial and scientific applications.^{5–8)} In addition, the doping of rare earth metals-doped to BaZrO₃ promotes a characteristic to be applied as a ion conductor^{9–12)} and phosphor.^{13–17)} BaZrO₃-based materials with perovskite structures are prepared by solid phase sintering systems^{1,9–12)} or spattering method.^{18,19)} On the other hand, it has recently been demonstrated that material feature of functional metal oxide fine particles is improved by control in exposed crystal planes even for the same crystal system.^{20–22)} Liquid-phase synthesis is one of the most powerful tools so as to prepare the size- and shape-controlled particles with a specific crystal plane. In this regard, extensive efforts have been carried out to obtain BaZrO₃ fine particles in hydrothermal,^{13,23,24)} solvothermal,^{25–27)} and sol-gel systems.^{7,28)} Lu *et al* reported that morphological control of BaZrO₃ microcrystal from rhombic dodecahedron to sphere is achieved with the adjustment of ethanol volume fraction in a hydrothermal synthesis.¹³⁾ However, hydrothermal synthesis of BaZrO₃ fine particles with narrow size distribution controlled in size has never been established so far. We have investigated to prepare well defined oxide fine particles precisely controlled in size and shape such as α-Fe₂O₃,^{29,30)} TiO₂,^{31–34)} SrTiO₃,^{35–37)} Bi_{0.5}Na_{0.5}TiO₃,^{38,39)} NaNbO₃,⁴⁰⁾ and K_{0.5}Nb_{0.5}NbO₃⁴¹⁾ with gel as an intermediate under highly concentrated hydrothermal conditions. The present research focused on to investigate novel hydrothermal synthesis of size- and shape-controlled BaZrO₃ fine particles under a highly condensed system. In this system,

a zirconium-triethanolamine (Zr-TEOA) complex, prepared by mixing tetra-*i*-propoxy zirconium and TEOA with the molar ratio of 1 : 2, was used as a Zr-source since TEOA ligand was coordinated with Ti⁴⁺ to form stable complexes against uncontrolled hydrolysis in our previous Ti-based particle synthesis.^{30–37)} As a result, sphere-, rhombic dodecahedral-, and flower-shaped BaZrO₃ fine particles were successfully obtained by the present method. Furthermore, the particle mean size of the sphere-shaped BaZrO₃ was precisely controlled by the control of the addition amount of NaOH. In the present study, we have also set our attention to investigate effect of particle size and shape and crystallinity of BaZrO₃-based phosphor powders on their fluorescence properties. Here, Europium was selected as a dopant because Europium-doped perovskite compounds are one of the most representative orange-colored phosphor materials. Up to date, Europium-doped BaZrO₃ (BaZrO₃:Eu) phosphor materials have been prepared mainly by solid phase sintering systems.^{42–45)} In such systems, precious control of particle mean size and shape is fundamentally difficult. Investigation to clarify fluorescence properties of hydrothermally prepared BaZrO₃:Eu powders controlled in size and shape might be expected to provide an important information about further design and synthesis of perovskite based phosphor materials.

2. Experimental

Reagent-grade barium hydroxide octahydrate (Ba(OH)₂·8H₂O: Cat. No: 024-00245) and TEOA (Cat. No: 145-05605) were purchased from Wako Pure Chemicals Ind. Co., Ltd.. Sodium hydroxide (NaOH: Cat. No: 3597401) and zirconium tetra-*i*-propoxide (Zr[OCH(CH₃)₂]₄: Cat. No: 335945), from Kojundo

Chemical Lab. Co., Ltd., were used for the BaZrO₃ synthesis. All reagents were used as received. Decarbonated water was prepared by argon-bubbling of double-distilled and ion-exchanged water using a glass ball filter (Kinoshita Rika Co., Ltd.) for 30 min under ultrasonic irradiation at room temperature. A Zr-TEOA aqueous solution was prepared as follows: Initially, Zr[OCH(CH₃)₂]₄ (16.4 g, 50 mmol) was well mixed with TEOA (14.9 g, 100 mmol) in a screw-capped Pyrex bottle under a dry N₂ atmosphere. Then, the mixture in the bottle was stirred at 60 °C for 24 hours in an oil bath. Then, decarbonated water was added into the glass bottle, and the total volume was adjusted to 100 mL using a measuring flask to make a pale yellow-colored aqueous stock solution of 0.50 mol/L in Zr⁴⁺. On the other hand, a Ba²⁺ aqueous solution (1.00 mol/L) was prepared as follows: Initially, Ba(OH)₂·8H₂O (15.8 g, 50 mmol) was dissolved in a hot water, and the total volume of the solution was adjusted to 50 mL by further addition of the hot water. Then, the resulting hot solution was filtered by a membrane filter (pore size: 0.45 μm) to remove insoluble white particulates. The representative procedure for the preparation of BaZrO₃ fine particle is as follows. The 1.00 mol/L Ba(OH)₂ aqueous solution (6.0 mL) was added to the same volume of the 0.50 mol/L Zr-TEOA aqueous solution in a Teflon-made screw-capped bottle, and the resulting mixture was well mixed at 60 °C with stirring in a water bath for 10 min. After aging at the same temperature for 1 h, 10 mL of the resulting white-colored suspension was transferred into a Teflon-lined autoclave (Parr Instrument Company, 4749) and aged at 250 °C for 3 h in an oven. The resulting white solid was collected by centrifugation (18,000 rpm, 10 min), and the sediments were washed for two times with an aqueous 0.50 mol/L acetic acid solution and three times with water by dispersing followed by centrifuging. The precipitates were dried at 60 °C in an oven. The yield was calculated from the weight of well-washed BaZrO₃. To investigate the effect of the aging temperature and period on the particle synthesis, the reaction temperature was changed from 100 to 250 °C and aged for different periods from 1 to 24 h. Effect of initial Zr⁴⁺ and Ba²⁺ concentrations on morphology of the BaZrO₃ fine particle was also studied by diluting 0.50 mol/L Zr-TEOA and 1.00 mol/L Ba(OH)₂ aqueous solutions with ion-exchanged and decarbonated water. On the other hand, size control of BaZrO₃ fine particles with a spherical shape was carried out by addition of NaOH into the initial Ba(OH)₂ solutions. The initial NaOH concentration in the Ba(OH)₂ solutions was changed from 0 to 2.0 mol/L. Here, 1.25 mol/L Ba(OH)₂ (4.8 mL) and 5.0–20 mol/L NaOH (1.2 mL) aqueous solutions were used for the control of NaOH concentration in the initial solutions. Furthermore, Europium-doping of the size- and shape-controlled BaZrO₃ fine particles were carried out by addition of Eu₂O₃ powder as the Eu³⁺ source. The addition amount of Eu³⁺ ions for doping was changed from 0.50 to 8.0 mol% based on the Zr⁴⁺ ions in the mixture of the Zr⁴⁺ and Ba²⁺ precursor solutions. Excess amount of Eu₂O₃ in the collected powders was removed by washing with 0.50 mol/L aqueous acetic solution (30 mL) at 60 °C for six times. The interval of the washing was 2 h.

X-ray diffraction (XRD) measurements were performed on a Rigaku Ultima-IV system using CuKα radiation (40 kV, 40 mA) equipped with a D/tEX Ultra detector. Scanning electron microscopic (SEM) images were taken by using a Hitachi SU-1510 system with the acceleration voltage of 10 kV. Transmission electron microscopic (TEM) observation was carried out by a Hitachi H-7650 at 100 kV. To determine the doping amount in a BaZrO₃ crystal structure, inductive coupled

plasma (ICP) measurements were carried out by a SPECTRO ARCOS system. Sample solutions for the ICP measurements were prepared by dissolving the 15 mg of the Eu-doped BaZrO₃ powders with a 2.0 mol/L HCl aqueous solution. The total volume of the solution was adjusted to 50 mL. Photoluminescence (PL) and its excitation (PLE) spectra were measured using a Hitachi fluorescence spectrophotometer F-2700 at room temperature.

3. Results and discussion

3.1. Effect of Ba/Zr molar ratio on formation of BaZrO₃ fine particles

Since the role of Ba(OH)₂ is the reservoir of the Ba source for BaZrO₃ as well as the basic compounds to increase pH, the effect of Ba/Zr on the particle formation was well investigated so as to obtain BaZrO₃ predominantly. In addition, the alkaline condition also affected the morphology of as-prepared fine particles, as reported for uniform TiO₂ particle formation.³⁴⁾ The initial concentration of the Zr-TEOA complex in the precursor mixture was fixed to 0.25 mol/L. The Ba/Zr molar ratio in the precursor mixture was adjusted to 0.50, 1.0, 1.5, and 2.0 by the adjustment of the initial Ba²⁺ concentration to 0.125, 0.25, 0.375, and 0.50 mol/L, respectively. The as-prepared solution mixture was aged at 250 °C for 3 h for the BaZrO₃ fine particle synthesis.

Figure 1 shows XRD patterns of solid particles formed with different initial Ba/Zr ratio. All diffraction peaks can be assigned as a cubic crystal phase of BaZrO₃ with lattice constants $a = 4.18 \text{ \AA}$ for all cases (JCPDS No. 01-089-2486). As shown in an inset of Figure 1a, broad peaks to the tetragonal ZrO₂ (JCPDS No.04-005-4212) is also found. ZrO₂ by-production was slightly observed at 1.0 in Ba/Zr ratio. The excess of Ba to stoichiometric ratio of Ba/Zr led to the formation of BaZrO₃ as a single phase. As SEM images of as-prepared particles are shown in Figure 2, the morphology was changed from sharp-edged and irregular-shape at 0.50 in Ba/Zr (Figure 2a) to a truncated rhombic dodecahedral shape¹³⁾ at 1.0 (Figure 2b). Both micron- and nano-sized particles with irregular shapes are observed in TEM images in insets in the

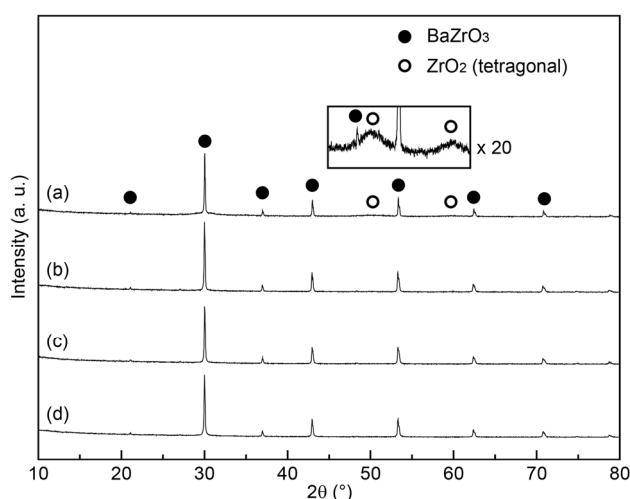


Fig. 1 XRD patterns of BaZrO₃ fine particles hydrothermally prepared by adjusting Ba/Zr molar ratio: (a) 0.50; (b) 1.0; (c) 1.5; (d) 2.0 (mol/mol). The reaction was carried out by aging at 60 °C for 1 h followed by heating at 250 °C for 3 h in a Teflon-lined autoclave.

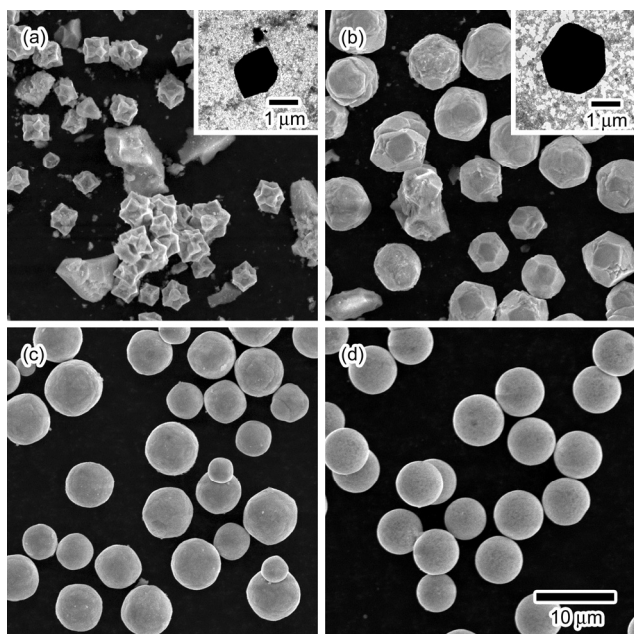


Fig. 2 SEM images of BaZrO₃ fine particles hydrothermally prepared by adjusting Ba/Zr molar ratio: (a) 0.50; (b) 1.0; (c) 1.5; (d) 2.0 (mol/mol). The scale bar in (d) is common for all images. The aging temperature was fixed at 250 °C and aged for 3 h. Insets in Fig. 2a and b shows the corresponding TEM images.

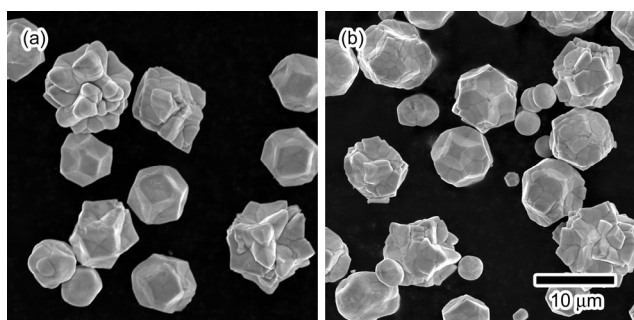


Fig. 3 SEM images of BaZrO₃ fine particles obtained under a hydrothermal condition. The reaction was carried out by pre-heated at 60 °C for 1 h followed by aging at 250 °C for 3 h using different Zr⁴⁺ sources as a precursor: (a) ZrOCl₂ and (b) ZrO(CH₃COO)₂. The scale bar in (b) is common for all images.

Figures 2a and 2b. Taking an XRD pattern (Figure 1a) into account, the micron- and the nano-sized particles could be assigned as BaZrO₃ and ZrO₂ particles, respectively. In contrast, in the case of the Ba/Zr molar ratios of 1.5 and 2.0, spherical BaZrO₃ fine particles are formed predominantly. The particle mean diameter with the size distribution of the BaZrO₃ spheres exhibited in Figures 2c and 2d are $5.7 \pm 1.2 \mu\text{m}$ and $6.0 \pm 0.8 \mu\text{m}$, respectively. The size distribution becomes narrow with increasing in the Ba/Zr molar ratio. In particular, highly monodispersed BaZrO₃ microspheres are obtained in the case of the initial Ba/Zr ratio of 2.0. In contrast, when ZrOCl₂, ZrO(NO₃)₂, or ZrO(CH₃COO)₂ was used as a zirconium source, irregularly-shaped and sharp-edged BaZrO₃ particles in a single phase, determined by XRD measurement, with large size distribution are formed for all cases (Figure 3). In these cases, unexpected white precipitates were observed in the initial solution mixture so that various kinds of metal ion complexes were included in the solution. Hence, the storing of specific monomer as a direct precursor solute to BaZrO₃ was not

controlled so as to separate the nucleation and particle growth stages.

3.2. Effect of aging temperature and periods on BaZrO₃ fine particles synthesis

To investigate effect of aging temperature and its period on the present BaZrO₃ fine particles synthesis, the precursor solution was aged in an autoclave at 100–250 °C for different aging period in the range from 1 to 24 h. Here, the initial Ba/Zr ratio was fixed to 2.0. Figure 4 shows SEM images of the representative solid particles obtained with different aging temperature and period. By XRD measurements, all the particles shown here could be assigned as a BaZrO₃ powders with a cubic crystal system in a single phase. The SEM observation revealed that the BaZrO₃ powders have a microsphere shape for all cases. This means that the aging temperature and the period are not fundamental factors for the shape control. Figure 5 shows change in BaZrO₃ yields with aging time at different temperature. Figure 5 also exhibits change in mean diameter of the BaZrO₃ microspheres, determined by count of 200 particles in the SEM images. No solid particulate was formed below 100 °C. The yield monotonously increases with aging time and reaches nearly

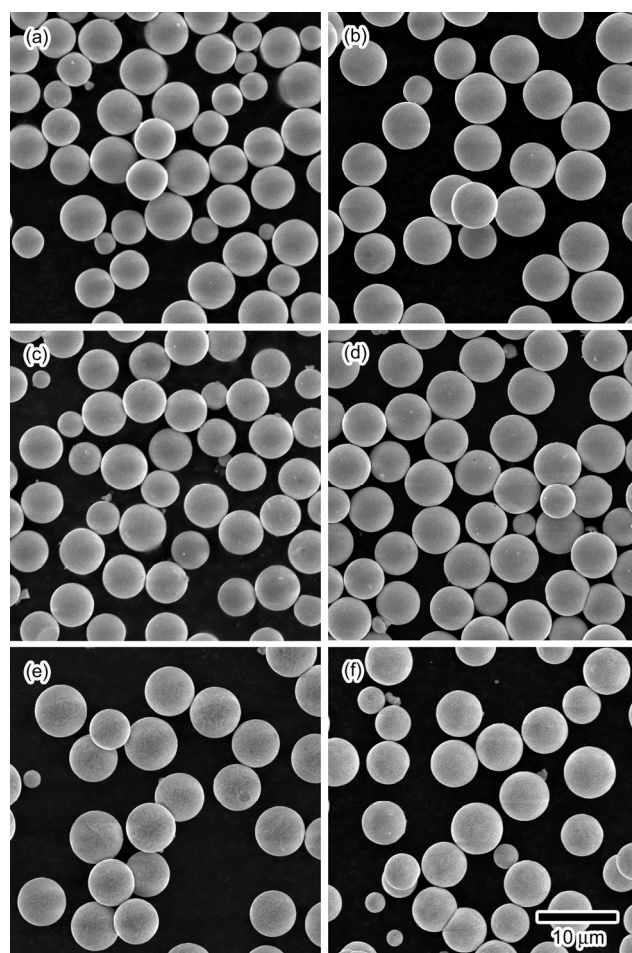


Fig. 4 SEM images of BaZrO₃ fine particles hydrothermally prepared by changing the heating temperature and the periods: (a) 150 °C, 3 h; (b) 150 °C, 6 h; (c) 200 °C, 1 h; (d) 200 °C, 3 h; (e) 250 °C, 1 h; (f) 250 °C, 24 h. The scale bar in (f) is common for all images. The initial Ba/Zr molar ratio was fixed to 2.0 for all cases.

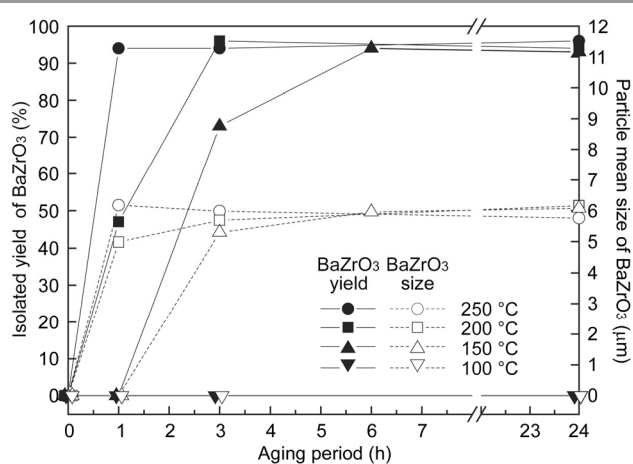


Fig. 5 Relationship between isolated yields and the particle mean sizes of BaZrO₃ particles prepared with different aging temperature and the periods.

100% at 6 h. Since the yield reaches *ca.* 100% at 3 h and 1 h for 200 °C and 250 °C, respectively, the temperature accelerated particle production. Particle mean diameter of BaZrO₃ converged at *ca.* 6 μm for 100% yield in the temperature range of 150 to 250 °C. In the present process, the Ostwald ripening²⁴⁾ is not a fundamental formation mechanism because of any further aging time effects on particle size after 100% yield. Namely, the uniform nucleation followed by the crystal growth to form basically single crystalline particles is the predominant reaction mechanism in the present process.

3.3. Shape control of BaZrO₃ fine particles: Effect of Ba²⁺ and Zr⁴⁺ concentrations

In the previous section, BaZrO₃ fine particles with a spherical shape were obtained for all cases. Next, we focused our attention on synthesis of BaZrO₃ fine particles controlled in shape. In general, fine particles with anisotropic shapes are obtained by adsorption of shape controller on specific crystal planes^{29, 30, 32-34)} or utilization of difference in the surface energies.⁴⁶⁾ In the latter case, deceleration of the particle growth is a practical way because kinetically-controlled fine particles surrounded by the specific surfaces are formed in such systems. To induce the kinetically-controlled system, we have investigated the effect of initial Zr⁴⁺ concentration. The initial Zr⁴⁺ concentration was changed in the range from 0.050 to 0.20 mol/L at the constant Ba/Zr molar ratio, 2.0, and aged at 250 °C for 3 h. XRD measurements of the solid particles collected after washing and drying revealed that all the white powders obtained under different initial Zr⁴⁺ concentration had a cubic BaZrO₃ crystal structure in a single phase for all cases.

Figure 6 shows the SEM images of as-prepared BaZrO₃ particles. Sharp-tipped flower-like particles are observed predominantly for 0.050 mol/L. (Figure 6a). The particle shape is changed into a truncated rhombic dodecahedral shape with increase in Zr⁴⁺ concentration to 0.10 and 0.15 mol/L (Figures 6b and 6c). Formation of such truncated rhombic dodecahedral shaped particles is derived from anisotropic evolution of {110} planes on the surfaces of the particles.¹³⁾ Further increase in the initial Zr⁴⁺ concentration to 0.20 mol/L affords the BaZrO₃ microspheres with the average diameter of 5.7 ± 0.7 μm (Figure 6d). The diameter is lower than that with the microspheres obtained with the initial Zr⁴⁺ concentration of 0.25 mol/L (Figure 2d). The difference in size might be derived from the difference of the total amount of the initial Ba²⁺ and Zr⁴⁺

sources in the reaction vessels. Evolution of anisotropic shapes such as the sharp-tipped flower and the truncated rhombic dodecahedral shapes observed only at the low initial Zr⁴⁺ concentrations. BaZrO₃ particles surrounded by unstable specific surfaces may be formed by the preferential growth along the specific direction regulated by the surface energy. Since Wang⁴⁶⁾ and Sun⁴⁷⁾ has reported that the surface energy of {110} planes of polyhedral crystals is higher than that of {100} and {111} planes, the truncated rhombic dodecahedral shapes with {110} planes on the surfaces of the particles were obtained in the present case.

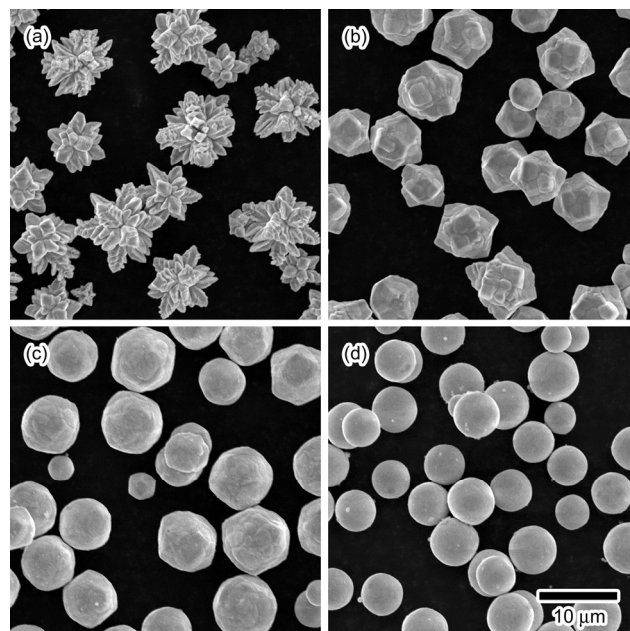


Fig. 6 SEM images of BaZrO₃ fine particles formed by changing the initial Ba²⁺ and Zr⁴⁺ concentration. The initial molar ratio of Ba/Zr was fixed to 2.0. (a) Zr⁴⁺ = 0.050 mol/L; (b) Zr⁴⁺ = 0.10 mol/L; (c) Zr⁴⁺ = 0.15 mol/L; (d) Zr⁴⁺ = 0.20 mol/L. The reaction was carried out by aging at 60 °C for 1 h followed by heating at 250 °C for 3 h in a Teflon-lined autoclave. The scale bar in (d) is common for all images.

3.4. Size control of BaZrO₃ fine particles: Effect of NaOH concentration

Effect of hydroxide ion concentration on the particle size was also investigated with change in NaOH concentration from 0 to 2.0 mol/L. As prepared samples were confirmed as BaZrO₃ over 90% yields in any case. Figure 7 exhibits SEM images of the BaZrO₃ powders formed with different initial NaOH concentration from 0.50 to 2.0 mol/L. The average particle mean size was gradually decreased from 4.3 to 2.4 μm with increase in NaOH concentration from 0.50 to 2.0 mol/L. In hydrothermal systems of simple metal oxide particle synthesis such as α-Fe₂O₃,⁴⁸⁾ nuclei number is generally increased with the increase in NaOH concentration because concentration of direct precursor for the nucleation is increased by increasing NaOH concentration. Such acceleration of the nucleation results in decreasing in particle mean size.⁴⁸⁾ However, in the case of liquid phase synthesis of complex metal oxide particles such as perovskite compounds, control of direct precursor concentrations of both A and B sites metal ions for the size control is quite difficult when the solubility of A and B sites ions in the growing solution is different. As mention in section 3.2, homogeneous nucleation and the successive particle growth is the unique route to give present BaZrO₃ microspheres.

Under such system, NaOH efficiently acted as size controller, and the particle mean size of BaZrO₃ is successfully controlled in the range from 2.5 ± 0.3 μm to 6.0 ± 0.8 μm keeping with the narrow size distribution.

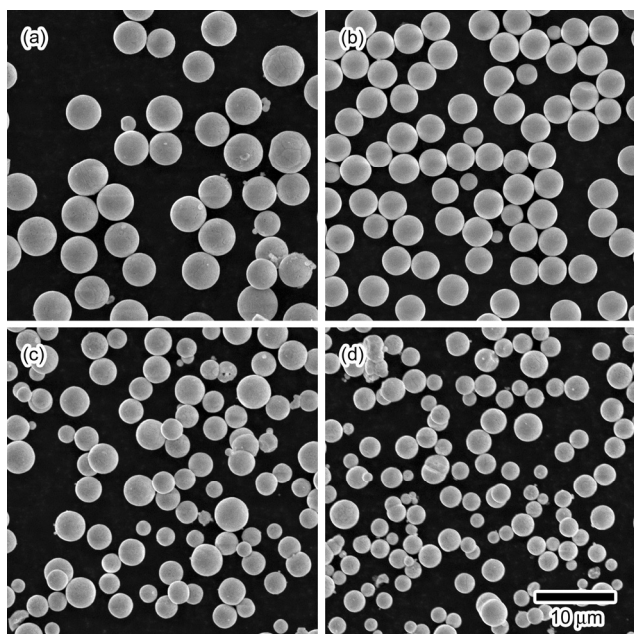


Fig. 7 SEM images of BaZrO₃ fine particles hydrothermally prepared with different initial NaOH concentration: (a) 0.50; (b) 1.0; (c) 1.5; (d) 2.0 mol/L. The reaction was carried out by pre-heated at 60 °C for 1 h followed by heating at 250 °C for 3 h in a Teflon-lined autoclave. The scale bar in (d) is common for all images.

3.5. Fluorescence behavior of Eu-doped BaZrO₃ controlled in size

In the previous section, BaZrO₃ microspheres controlled in size in the range from 2.5 ± 0.3 μm to 6.0 ± 0.8 μm keeping with the narrow size distribution. By applying the system, we have investigated the effect of particle mean size on the PL property of BaZrO₃-based phosphor powders by Europium doping. The Eu-doping was carried out by mixing Eu₂O₃ powder into the initial mixed aqueous solution of Ba(OH)₂ and the Zr-TEOA complex, as described in the Experimental section. When the mixing amount of Eu³⁺ ions was changed from 2.0 to 8.0 mol% based on the Zr⁴⁺ ions, un-doped Eu₂O₃ crystal phase was seen by XRD measurement even if the thorough washing with a 0.5 mol/L acetic acid aqueous solution at 60 °C. In contrast, when the mixing amount was fixed to 0.50 and 1.0 mol%, a BaZrO₃ phase was observed as a single phase after the washing. The doping amounts in the BaZrO₃ crystal structure could be determined as 0.18 and 0.51 mol%, respectively, by the ICP measurement (based on Zr⁴⁺ ions). Although the doping amount was lower than that of the initial mixing ratio, it could be controlled by the control of the initial mixing amount of Eu₂O₃ powder in the range from 0 to 1.0 mol% Eu³⁺ ions based on the Zr ions. On the other hand, further addition of Eu₂O₃ resulted in remaining of the Eu₂O₃ in the BaZrO₃:Eu powders. In this regard, we could set maximum doping amount of Eu³⁺ ions in the present study as about 0.5 mol%, and abbreviated as BaZrO₃:Eu_{0.005}.

To investigate the effect of particle mean size on the PL property under constant 1.0 mol% Eu³⁺ ions to Zr⁴⁺ ones, the particle mean size was controlled by the addition of NaOH as mentioned in section 3.4, varying from 0 to 2.0 mol/L. The ICP measurements revealed that the doping amounts of Eu³⁺ ions in the BaZrO₃ crystal structure were 0.5 mol% for all cases (based on Zr ions). The initial NaOH concentration did not influence the maximum doping efficiency in the present system. The particle mean diameter with the size distribution of the BaZrO₃:Eu_{0.005} microspheres obtained with 0, 0.50, 1.0, 1.5, and 2.0 mol/L NaOH was 5.4 ± 0.7, 4.2 ± 0.5, 3.7 ± 0.6, 3.4 ± 0.5, and 2.5 ± 0.3 μm, respectively. As a result, highly uniformed BaZrO₃:Eu_{0.005} microspheres controlled in size were successfully obtained. Due to the difference of the ion sizes between Ba²⁺ (0.135 nm) and Zr⁴⁺ (0.072 nm), Eu³⁺ ions (0.095 nm) are expected to substitute for the Zr⁴⁺ sites in the BaZrO₃ lattice.

Figures 8a and 8b show room temperature PLE and PL spectra of the BaZrO₃:Eu_{0.005} microspheres with different in size. The PLE spectra are monitored by an emission wavelength (λ_{em}) of 596 nm (a ⁵D₀-⁷F₁ emission band of Eu³⁺). A broad excitation band at 230-260 nm in the PLE spectra is found. The band is known to be a charge-transfer process from oxygen 2p orbital to an empty 4f orbital of Eu³⁺.⁴⁹ The maximum peak position of the PLE spectra is slightly blue-shifted when the particle mean size is decreased. The excitation wavelength (λ_{ex}) for the PL spectra, shown in Figure 8b, was fixed to 248, 247, 247, 247, and 245 nm for the microspheres with the different average size of 5.4, 4.2, 3.7, 3.4, and 2.5 μm, respectively. All powders show peaks at 580, 596, 613, and 650-660 nm (broad), which are assigned to ⁵D₀-⁷F₀, ⁵D₀-⁷F₁, ⁵D₀-⁷F₂, and ⁵D₀-⁷F₃ transitions of Eu³⁺ ions, respectively.⁴⁹ The peak positions well matched in spite of the difference in the particle mean size. On the other hand, decrease in the maximum ⁵D₀-⁷F₁ emission

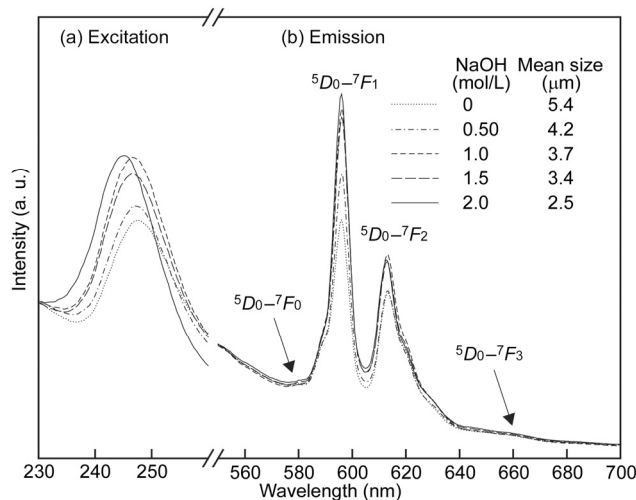


Fig. 8 PLE and PL spectra of BaZrO₃:Eu_{0.005} microspheres with different in size. The emission wavelength of the PLE spectra was fixed to 596 nm. The λ_{ex} for the PL spectra was set to 248, 247, 247, 247, and 245 nm for the microspheres with the different average size of 5.4, 4.2, 3.7, 3.4 and 2.5 μm, respectively. The doping amount of Eu³⁺ ions was 0.5 mol% based on Zr⁴⁺ ions.

intensity is observed by the increase of the size from 3.7 to 5.4 μm . Such decrease in the PL intensity might be derived from increase of light scattering effect from the phosphor microspheres by increasing the particle mean size.

3.6. Effects of particle shape and crystallinity of Eu-doped BaZrO₃ on the fluorescence behavior

Next, effect of particle shape on the PL behavior has been also investigated. Figure 9 exhibits room temperature PLE and PL spectra of the Eu-doped BaZrO₃:Eu particles with a spherical and a dodecahedral shapes. SEM images of the particles are shown in the insets of Figure 9. The Eu-doped BaZrO₃ with the rhombic dodecahedral shape was prepared by the same procedure for the preparation of the particles shown in Figure 6b. In this case, the initial mixing amount of Eu³⁺ ions was fixed to 1.0 mol% based on the Zr⁴⁺ ions by the addition of Eu₂O₃ powder. The doping amount of Eu³⁺ ions in the BaZrO₃ crystal structure was checked by ICP measurements, and assigned as 0.13 mol% (abbreviated as BaZrO₃:Eu_{0.0013}). The particle mean diameter of the BaZrO₃:Eu_{0.0013} particles with the dodecahedral shape was 5.9 μm . In general, PL intensity is strongly influenced by the doping amount of rare earth metals in the host crystal. Further, to investigate the effect of shape on the PL behavior in detail, it should be compared using the same-sized particles with different morphology. In this regard, we have prepared BaZrO₃:Eu_{0.0013} microspheres with 5.9 μm in size by the optimization of the initial mixing amount of Eu₂O₃ powder. As a result, the BaZrO₃:Eu_{0.0013} microspheres exhibited in the inset of Figure 9 were obtained. The optimized initial mixing amount of Eu³⁺ ions was 0.40 mol% based on the Zr⁴⁺ ions. On the other hand, in spite of the extensive effort, Eu-doping into the sharp-tipped flower-like particles exhibited in Figure 6a was unsuccessful.

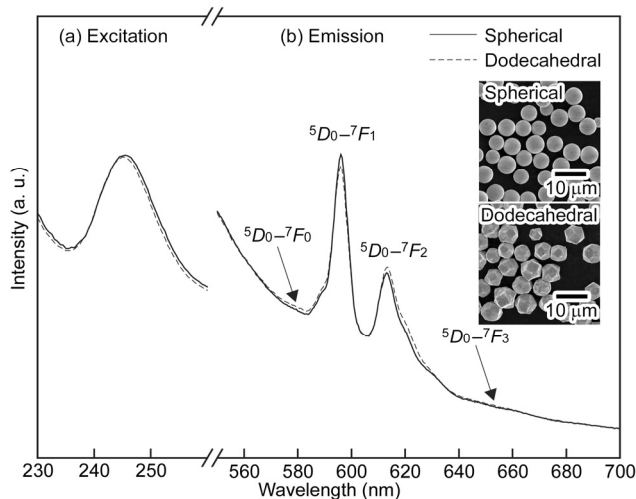


Fig. 9 PLE and PL spectra of BaZrO₃:Eu_{0.0013} phosphors with a spherical and a dodecahedral shape. The λ_{em} and λ_{ex} were 596 and 249 nm, respectively. The doping amount of Eu³⁺ was 0.13 mol% based on Zr⁴⁺.

Figure 9a shows the PLE spectra of spherical- and dodecahedral-shaped BaZrO₃:Eu_{0.0013} powders. The emission wavelength (λ_{em}) was set to 596 nm. As described in Figure 8, a

broad excitation band at 230–260 nm, corresponding to a charge transfer from oxygen 2p orbital to an empty 4f orbital of Eu³⁺, is also observed. The intensity as well as the pattern of the PLE spectra is almost same with both of the cases. Figure 9b is the PL spectra of the shape-controlled powders. The λ_{ex} was fixed to 249 nm. Two strong emission peaks at 596 and 613 nm corresponding to ⁵D₀–⁷F₁ and ⁵D₀–⁷F₂ transitions of Eu³⁺, respectively, are seen in Figure 9b. It has already been reported that the PL peaks are sensitive to the symmetry around Eu³⁺ ions, and strongly influenced by the outside surroundings of Eu³⁺ ions. Here, the ⁵D₀–⁷F₂, corresponding to electric-dipole transition, is only allowed when Eu³⁺ ions are embedded at a site of non-inversion symmetry.⁵⁰ On the other hand, the ⁵D₀–⁷F₁, corresponding to electric-dipole transition, is allowed when Eu³⁺ ions are occupied at a site of inversion symmetry. This means that the PL intensity ratio of ⁵D₀–⁷F₂ to ⁵D₀–⁷F₁, can be called as asymmetry ratio, provides the degree of distortion from inversion symmetry of the local environment around the Eu³⁺ ions in the host crystal.⁵⁰ In Figure 9b, the intensity ratio of the BaZrO₃:Eu_{0.0013} phosphors with spherical and dodecahedral shapes is 0.51 and 0.57, respectively. It should be noteworthy that these intensity ratios are quite lower than that of the previously reported Eu-doped inorganic phosphor powders obtained under solution systems such as BaZrO₃,¹³ MSnO₃ (M = Ca, Sr, and Ba),⁵¹ BaTiO₃,⁵² CaZrO₃,⁵³ and RE₂O₃ (RE = La, Gd, and Y etc.)⁵⁴. The result indicated that the symmetry around Eu³⁺ ions of the present system is extremely higher than that of the previous systems.^{13,51–54} The reason why such behavior observed in the present report is that the particles obtained in the present system might be basically single crystalline. In fact, BaZrO₃:Eu phosphors with such low asymmetry ratio is generally obtained by way of high temperature sintering to increase its crystallinity.⁵⁵ The asymmetry ratio of the particles with the dodecahedral shape is slightly higher than that with the spherical shape. As described in section 3.3, the dodecahedral shaped particles have {110} planes with high surface energy on its surfaces. Decrease in the symmetry around the Eu³⁺ ions might be due to evolution of the specific {110} planes. Further precious shape control might be an effective tool for fine tuning the emission wavelength of phosphor materials.

4. Conclusions

In the present study, BaZrO₃ fine particles controlled in their size and shape were successfully prepared by a hydrothermal method starting from barium hydroxide and a Zr⁴⁺-TEOA complex as water-soluble precursors. BaZrO₃ microspheres with a cubic crystal structure were formed in a single phase with initial Ba/Zr molar ratios of 1.5 and 2.0. The size distribution of the microspheres obtained in the case with the initial Ba/Zr ratio of 2.0 was 6.0 ± 0.8 μm , monodispersed BaZrO₃ microspheres are obtained for the first time. Investigation about the formation mechanism revealed that uniform nucleation followed by the crystal growth to form basically single crystalline particles is the predominant reaction mechanism in the present system. The particles shape was drastically changed from the spherical shape to a truncated dodecahedral or a flower-like shape by the change of the initial Ba²⁺ and Zr⁴⁺ concentrations (the Ba/Zr molar ratio was fixed to 2.0). Evolution of such anisotropic shapes might be induced when the supply rate of Ba²⁺ and Zr⁴⁺ ions was the rate-determining step of the particle growth. The particle mean size of the BaZrO₃ microspheres was also gradually controlled by

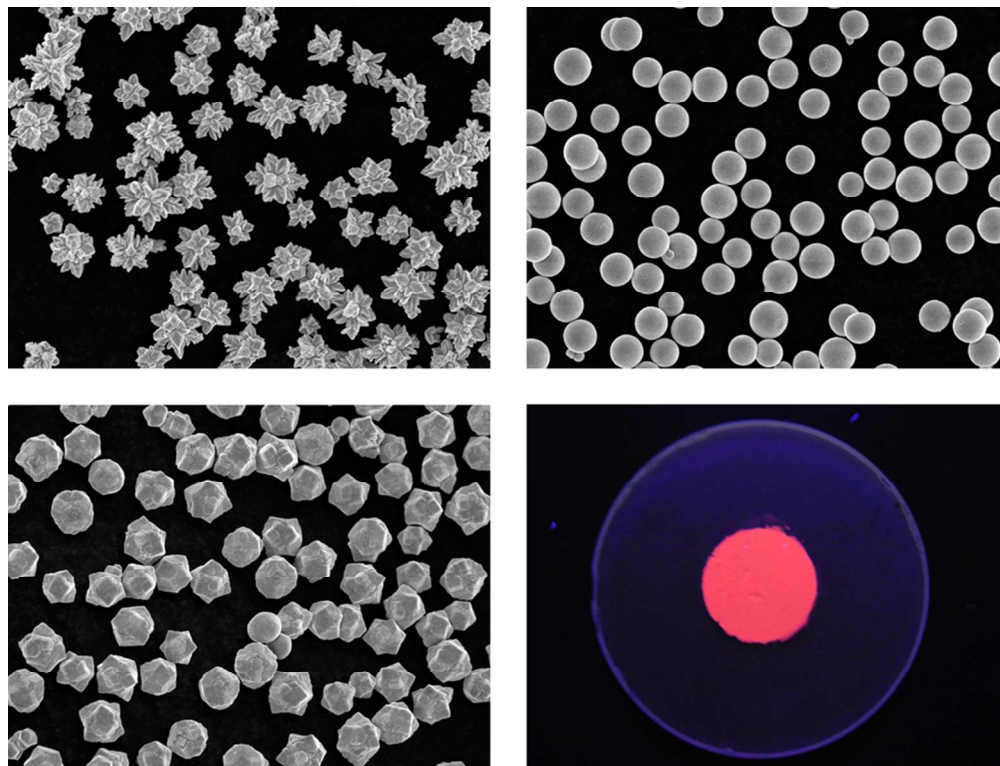
the addition of NaOH in the range from 2.4 to 6.0 μm . Furthermore, we have applied the present system to investigate effect of size and shape of BaZrO₃:Eu powders on their PL property. The emission intensity of the microspheres was influenced by the size. Decrease in the PL intensity by the increase of the particle mean size might be derived from increase of light scattering effect from the phosphor microspheres. Further, the asymmetric ratio of the photoluminescence intensity of the resulting BaZrO₃:Eu powders suggested the particles obtained by the present method had a basically single crystalline structure. Further, the asymmetry ratio of the particles with the dodecahedral shape is slightly higher than that with the spherical shape. Further studies focusing on precious shape control might be an effective tool to develop emission colour-tuneable phosphor materials.

Notes and references

^a Institute of Multidisciplinary Research for Advanced Materials, Tohoku University, 2-1-1 Katahira, Aoba-ku, Sendai, Miyagi, 980-8577, Japan. E-mail: kanie@tagen.tohoku.ac.jp; Tel.: +81-22-217-5165.

- R. Vassen, X. Cao, F. Tietz, D. Basu and D. Stöver, *J. Am. Ceram. Soc.*, 2000, **83**, 2023.
- J. Robertson, *J. Vac. Sci. Technol. B*, 2000, **18**, 1785.
- A. R. Akbarzadeh, I. Kornev, C. Malibert, L. Bellaiche and J. M. Kiat, *Phys. Rev. B*, 2005, **72**, 205104.
- J. W. Bennett, I. Grinberg and A. M. Rappe, *Phys. Rev. B*, 2006, **73**, 180102.
- G. Lupina, O. Seifarth, G. Kozłowski, P. Dudek, J. Dąbroeski, G. Lippert and H. -J. Müssig, *Microelectron. Eng.*, 2009, **86**, 1842.
- Y. Yuan, X. Zhang, L. Liu, X. Jiang, J. Lu, Z. Li and Z. Zou, *Int. J. Hydrogen. Energy*, 2008, **33**, 5941.
- N. Prastomo, N. H. B. Zakaria, G. Kawamura, H. Muto, M. Sakai and A. Matsuda, *J. Eur. Ceram. Soc.*, 2011, **31**, 2699.
- A. Erb, E. Walker and R. Flükiger, *Physica C*, 1995, **245**, 245.
- H. Iwahara, T. Yajima, T. Hibino, K. Ozaki and H. Suzuki, *Solid State Ionics*, 1993, **61**, 65.
- R. C. T. Slade, S. D. Flint and N. Singh, *Solid State Ionics*, 1995, **82**, 135.
- H. G. Bohn and T. Schober, *J. Am. Ceram. Soc.*, 2000, **83**, 768.
- F. Iguchi, Y. Nagao, N. Sata and H. Yugami, *Solid State Ionics*, 2011, **192**, 97.
- Z. Lu, Y. Tang, L. Chen and Y. Li, *J. Cryst. Growth*, 2004, **266**, 539.
- J. Oliva, E. de la Rosa, L. A. Diaz-Torres, P. Salas and C. Ángeles-Chavez, *J. Appl. Phys.*, 2008, **104**, 023505.
- H. Zhou, Y. Mao and S. S. Wong, *J. Mater. Chem.*, 2007, **17**, 1707.
- L. Guo, X. Wang, C. Zhong and L. Li, *J. Am. Ceram. Soc.*, 2011, **94**, 3175.
- B. Mafi, K. C. Singh, M. Sahal, S. P. Khatkar, V. B. Taxak and M. Kumar, *J. Lumin.*, 2010, **130**, 2128.
- X. X. Chen, L. Rieth, M. S. Miller and F. Solzbacher, *Sensor Actuat B-Chem*, 2009, **142**, 166.
- R. Pornprasertsuk, O. Kosasang, K. Somroop, M. Horprathum, P. Limnonthakul, P. Chindaudom and S. Jinawath, *Solid State Sci.*, 2011, **13**, 1429.
- H. G. Yang, G. H. Sun, S. Z. Qiao, J. Zou, G. Liu, S. C. Smith, H. M. Cheng and G. Q. Lu, *Nature*, 2008, **453**, 638.
- T. Kimijima, T. Sasaki, M. Nakaya, K. Kanie and A. Muramatsu, *Chem. Lett.*, 2010, **39**, 1080.
- B. Hai, A. K. Shukla, H. Duncan and G. Chen, *J. Mater. Chem. A*, 2013, **1**, 759.
- A. Dias and V. S. T. Ciminelli, *Chem. Mater.*, 2003, **15**, 1344.
- Z. Dong, T. Ye, Y. Zhao, J. Yu, F. Wang, L. Zhang, X. Wang and S. Guo, *J. Mater. Chem.*, 2011, **21**, 5978.
- M. Niederberger, N. Pinna, J. Polleux and M. Antonietti, *Angew. Chem. Int. Ed.*, 2004, **43**, 2270.
- K. Nakashima, T. Goto, S. Iwatsuki, M. Kera, I. Fujii and S. Wada, *Mater. Sci. Eng.*, 2011, **18**, 092049.
- K. Nakashima, I. Fujii and S. Wada, *J. Ceram. Soc. Jpn.*, 2011, **119**, 532.
- M. Veith, S. Mathur, N. Lecerf, V. Huch, T. Decker, H. P. Beck, W. Eiser and R. Haberkorn, *J. Sol-Gel Sci. Technol.*, 2000, **15**, 145.
- T. Sugimoto, M. M. Khan and A. Muramatsu, *Colloids Surf. A: Physicochem. Eng. Asp.*, 1993, **70**, 167.
- T. Sugimoto, M. M. Khan, A. Muramatsu and H. Itoh, *Colloids Surf. A: Physicochem. Eng. Asp.*, 1993, **79**, 233.
- T. Sugimoto, K. Okada and H. Itoh, *J. Colloid Interface Sci.*, 1997, **193**, 140.
- T. Sugimoto, K. Okada and H. Itoh, *J. Disp. Sci. Technol.*, 1998, **19**, 143.
- T. Sugimoto, X. Zhou and A. Muramatsu, *J. Colloid Interface Sci.*, 2003, **259**, 53.
- K. Kanie and T. Sugimoto, *Chem. Commun.*, 2004, 1584.
- J. Cuya, N. Sato, K. Yamamoto, H. Takahashi and A. Muramatsu, *Thermochim. Acta*, 2004, **419**, 215.
- T. Kimijima, K. Kanie, M. Nakaya and A. Muramatsu, *Appl. Catal. B: Env.*, 2014, **144**, 462.
- T. Kimijima, K. Kanie, M. Nakaya and A. Muramatsu, *Mater. Trans.*, 2014, **55**, 147.
- K. Kanie, H. Sakai, J. Tani, H. Takahashi and A. Muramatsu, *Mater. Trans.*, 2007, **48**, 2174.
- K. Kanie, Y. Numamoto, S. Tsukamoto, T. Sasaki, M. Nakaya, J. Tani, H. Takahashi and A. Muramatsu, *Mater. Trans.*, 2011, **52**, 1396.
- K. Kanie, Y. Numamoto, S. Tsukamoto, H. Takahashi, H. Mizutani, A. Terabe, M. Nakaya, J. Tani and A. Muramatsu, *Mater. Trans.*, 2011, **52**, 2119.
- K. Kanie, H. Mizutani, A. Terabe, Y. Numamoto, S. Tsukamoto, H. Takahashi, M. Nakaya, J. Tani and A. Muramatsu, *Jpn. J. Appl. Phys.*, 2011, **50**, 09ND09.
- L. Guan, L. Jin, S. Guo, Y. Liu, X. Li, Q. Quo, Z. Yang and G. Fu, *J. Rare Earths*, 2010, **28**, 292.
- J. Huang, L. Zhou, Z. Wang, Y. Lan, Z. Tong, F. Gong, J. Sun and L. Li, *J. Alloy. Compd.*, 2009, **487**, L5.
- X. Liu and X. Wang, *Opt. Mater.*, 2007, **30**, 626.
- J. Alarcon, D. van der Voort and G. Blasse, *Mater. Res. Bull.*, 1992, **27**, 467.
- Z. L. Wang, *J. Phys. Chem. B*, 2000, **104**, 1153.
- Y. Sun and Y. Xia, *Science*, 2002, **298**, 2176.
- T. Sugimoto, S. Waki, H. Itoh and A. Muramatsu, *Colloids Surf. A: Physicochem. Eng. Asp.*, 1996, **109**, 155.
- G. Blasse and B. C. Grabmaier, *Luminescent Materials*, Springer, Berlin, 1994.
- T. Nogami, T. Enomoto and T. Hayakawa, *J. Lumin.*, 2002, **97**, 147.

- 51 Z. Lu, L. Chen, Y. Tang and Y. Li, *J. Alloy. Compd.*, 2005, **387**, L1.
- 52 M. García-Hernández, G. Chadeyron, D. Boyer, A. Garcia-Murillo, F. Carillo-Romo and R. Mahiou, *Nano-Micro Lett.*, 2013, **5** (1), 57.
- 53 H. Zhang, X. Fu, S. Niu and Q. Xin, *J. Alloy. Compd.*, 2008, **459**, 103.
- 54 D. Wang, Z. Wang, P. Zhao, W. Zheng, Q. Peng, L. Liu, X. Chen and Y. Li: *Chem. Asian. J.*, 2010, **5**, 925.
- 55 D. Sun, D. Li, Z. Zhu, J. Xiao, Z. Tao and W. Liu, *Opt. Mater.*, 2012, **34**, 1890.



82x62mm (300 x 300 DPI)